Supporting Information for

Climatic and landscape controls of regional streamflow variability across Peninsular India via the flow duration curve

Pankaj Dey[1], Jeenu Mathai[2], Murugesu Sivapalan[3,4] and Pradeep. P. Mujumdar[5,6]

[1]Department of Hydrology, Indian Institute of Technology, Roorkee, India

[2]National Centre for Earth Science Studies, Thiruvananthapuram, India

[3]Department of Civil and Environmental Engineering, University of Illinois at Urbana-Champaign, Urbana, IL, USA

[4]Department of Geography and Geographic Information Science, University of Illinois at Urbana-Champaign, Urbana, IL, USA

[5]Department of Civil Engineering, Indian Institute of Science, Bangalore, India

[6]Interdisciplinary Centre for Water Research, Indian Institute of Science, Bangalore, India

Contents of this file

Figures S1 to S11
Text S1-S2

This file contains eleven figures and two text paragraphs supporting the results presented in the main manuscript. The details of the figures are provided in the captions.
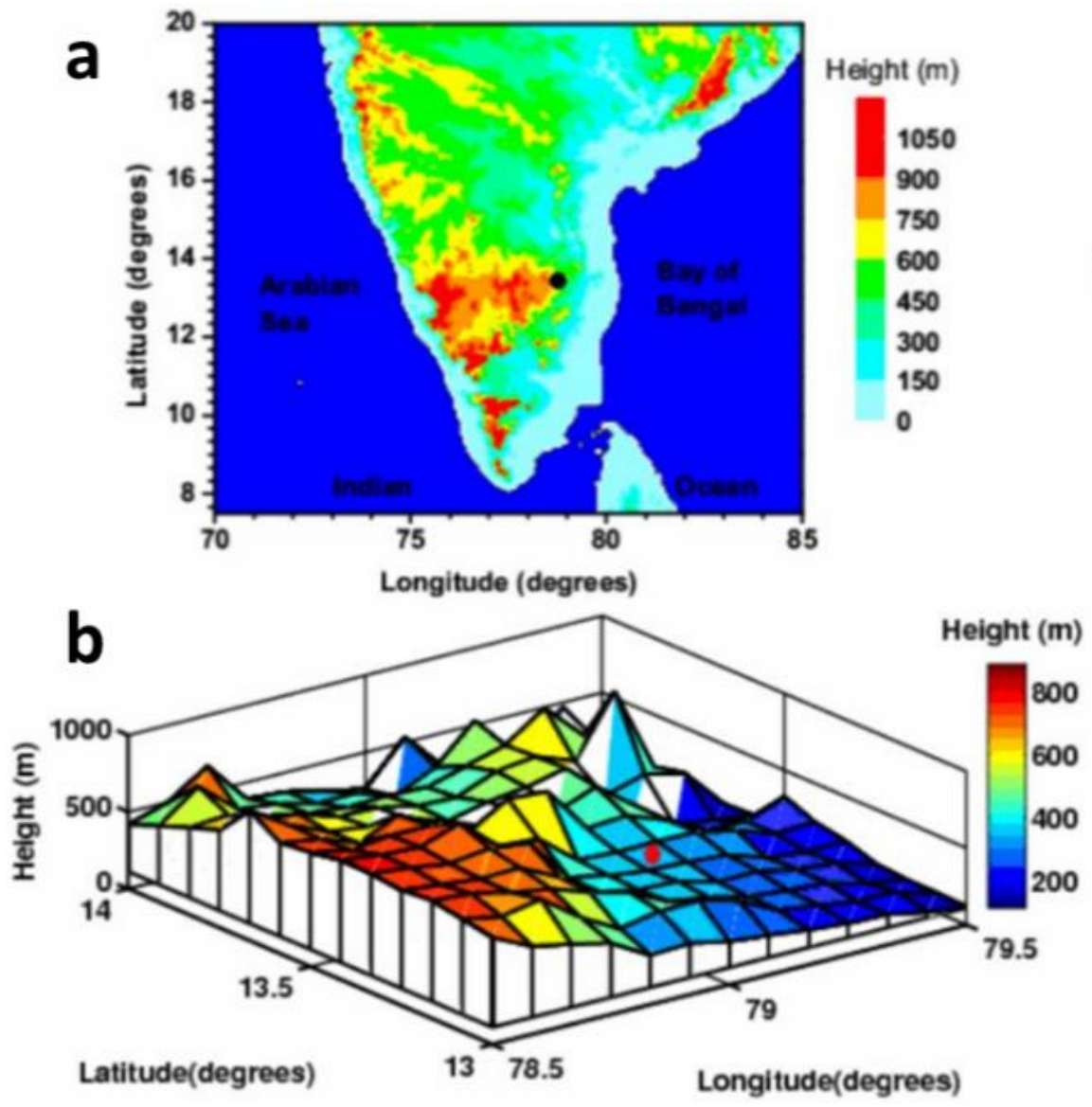
Figure S1. (a) Topography map of Peninsular region. The black circle represents the location of Gadanki in the Peninsular system [Reprinted from: (Jayaraman et al., 2010)] (b) High-resolution topography map for 50 km radius around the selected location of Gadanki [Reprinted from: (Jayaraman et al., 2010)].
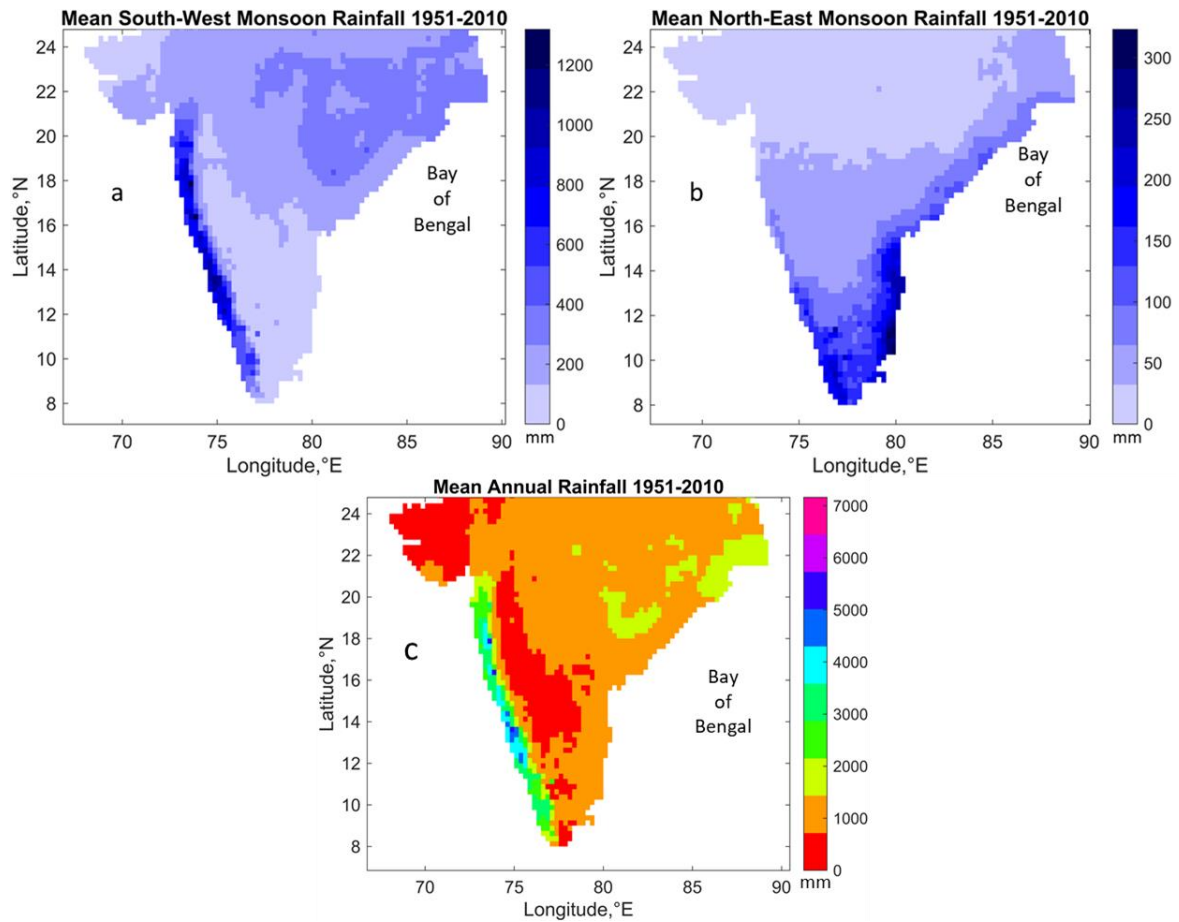
Figure S2: Spatial variation of South-West, North-East monsoon and annual rainfall in Peninsular India. The South-West monsoon (a) causes heavy rainfall along the Western Ghats. After crossing the Western Ghats, the rainfall reduces towards north-west direction. The low pressure systems which is caused due to synoptic-scale tropical disturbances formed over Bay of Bengal, moves in north-western direction towards mainland India. This low pressure systems brings significant amount of rainfall over the central India (Krishnamurthy & Ajayamohan, 2010; Prakash et al., 2015). The North-East monsoon (b) rainfall occurs mostly in the southern part of Peninsular region. The influence of both South-West and North-East monsoons introduce a bimodal seasonal patterns in monthly rainfall in the southern part of the Peninsular region.
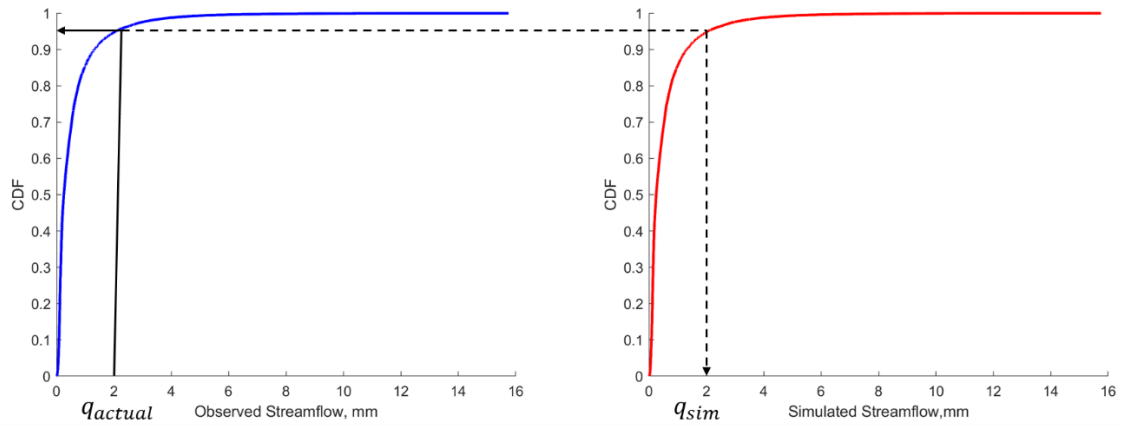
Figure S3. Estimation of q_{sim} using constructed annual CDF. The non-exceedance probability (denoted by CDF – shown in continuous black line) corresponding to actual streamflow (q_{actual}) is used to estimate the q_{sim} based on the constructed annual CDF (shown in dashed black line). The CDF corresponding to q_{sim} is developed based on equation 6.
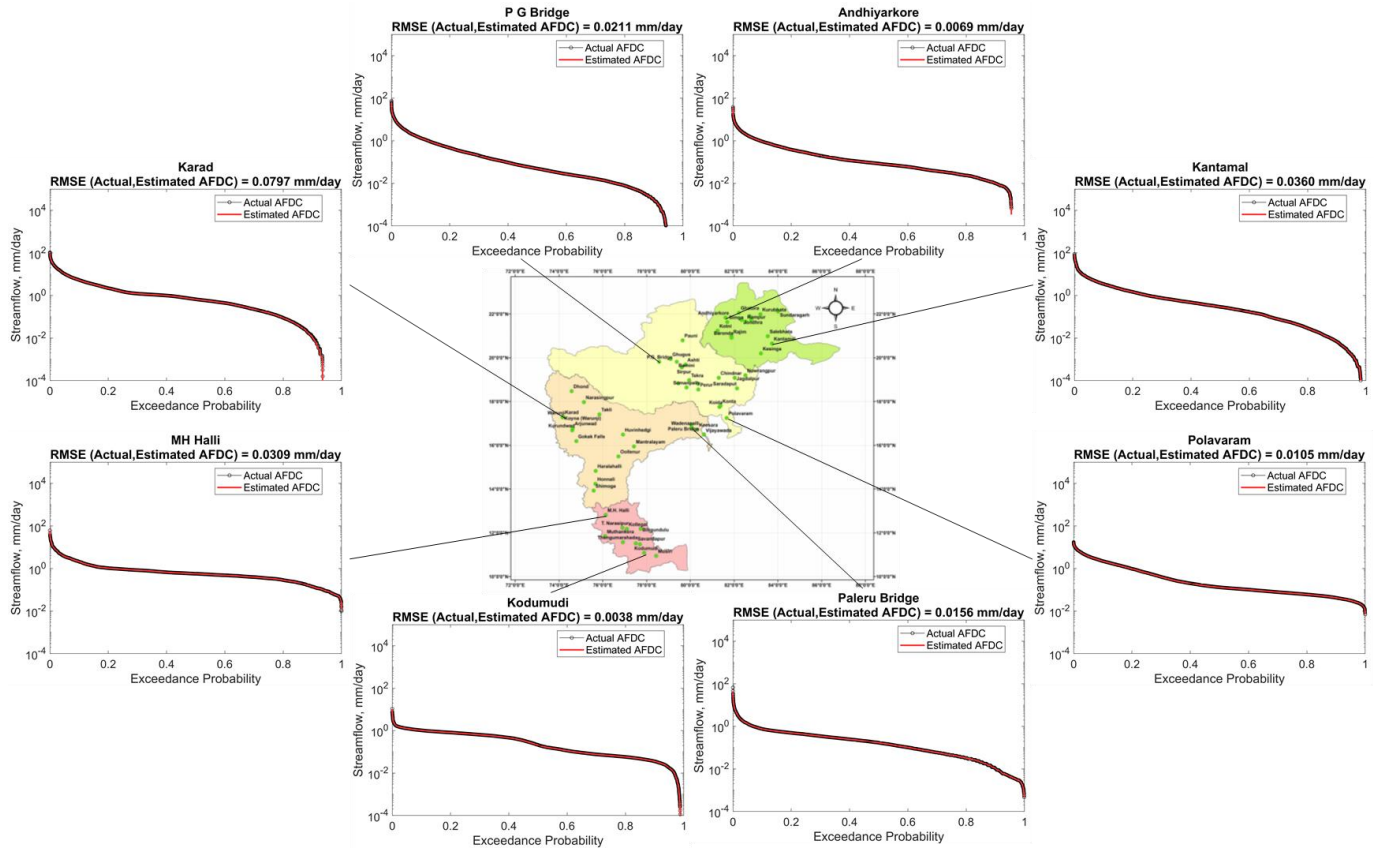
Figure S4: Performance of time scale partitioning framework for monthly flows in approximating the annual flow duration curve.
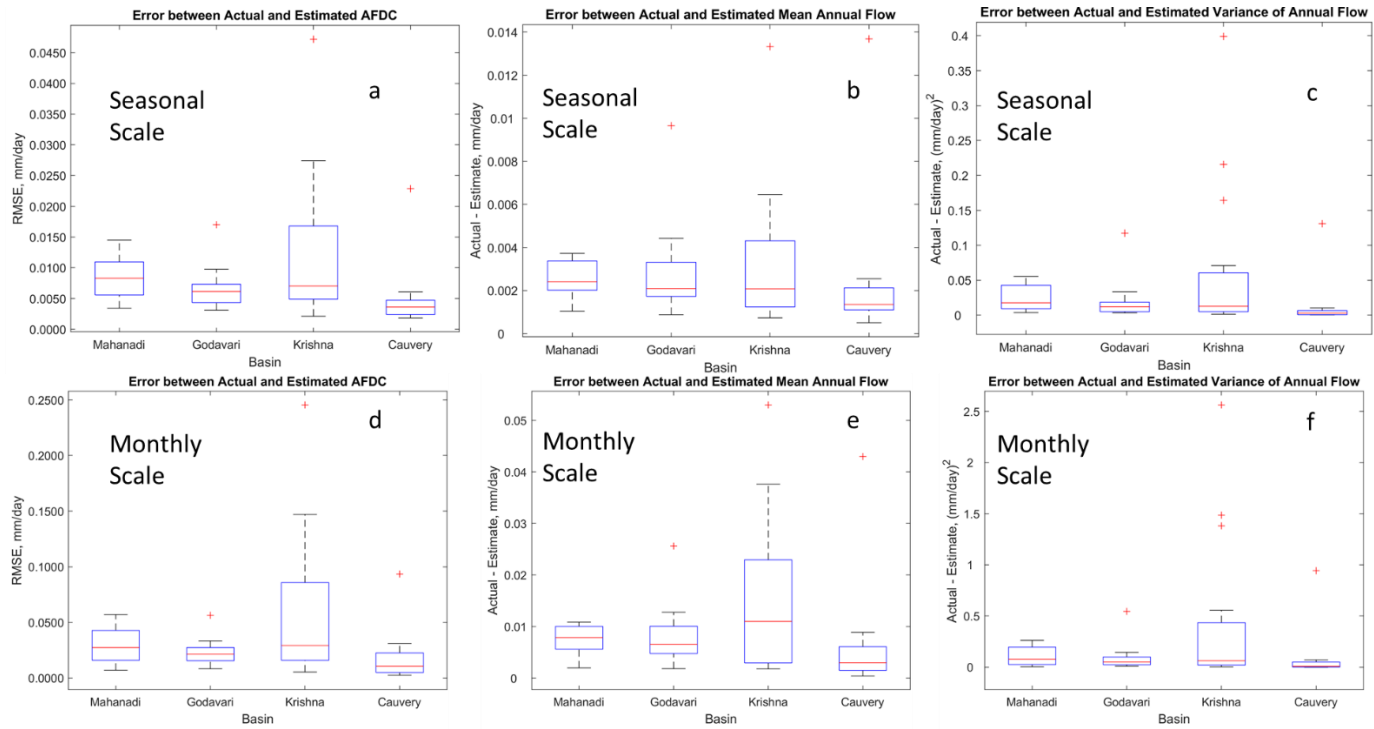
Figure S5: Performance of seasonal and monthly time scale partitioning of streamflow in approximating annual flow duration curve (a and d) and estimation of mean (b and e) and variance (c and f) of annual streamflow. The performances of seasonal time scale partitioning in approximating annual flow duration curve and estimation of mean and variance of annual streamflow are better than the monthly time scale partitioning. This may be due to the influence of longer duration in seasons which considers intra-seasonal carry over flows during monsoons. At monthly time scale, the carry over flows across different months are not considered in the framework.
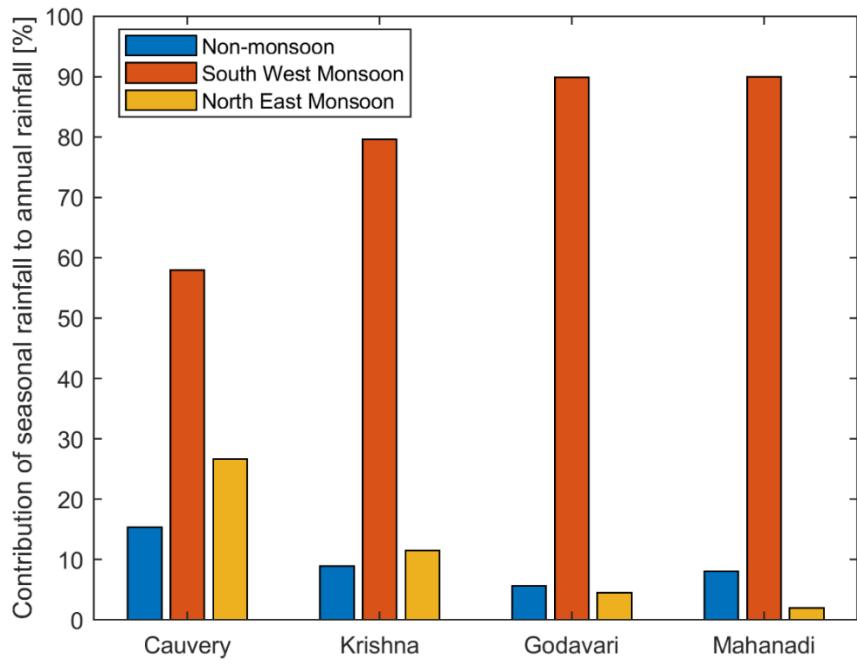
Figure S6. Contributions of seasonal rainfall to annual rainfall for long-term (1951-2010) period.

S1 Independence between flows across seasons:

The multivariate Hoeffding test (Gaißer et al., 2010) is conducted to check the independence between three random variables representing Non-monsoon, South West Monsoon and North East Monsoon flows respectively. A value of test statistic – φ^2 – close to zero indicates independence between three random variables. It is observed that except for two stations in Krishna basin, 60 out of 62 stations are showing independence between flows across seasons (Figure S7). Therefore, the assumption of no carry-over is used to construct annual FDC based on seasonal FDCs.
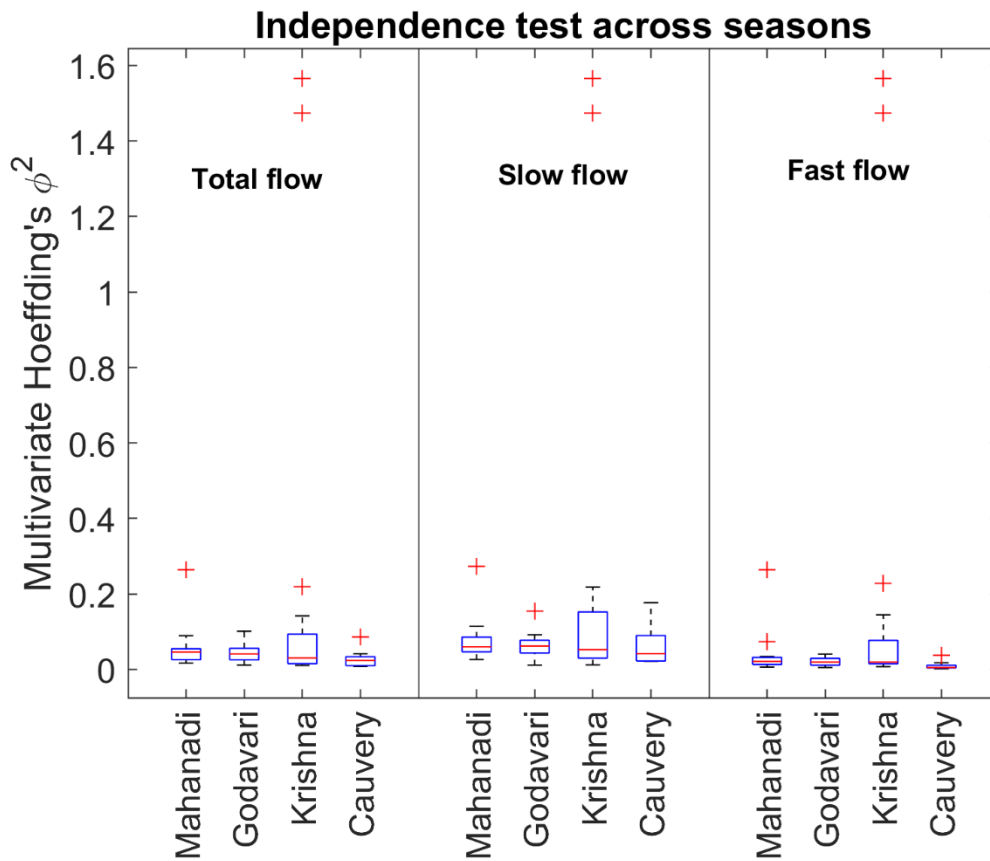
Figure S7: Test of independence across seasonal flows.
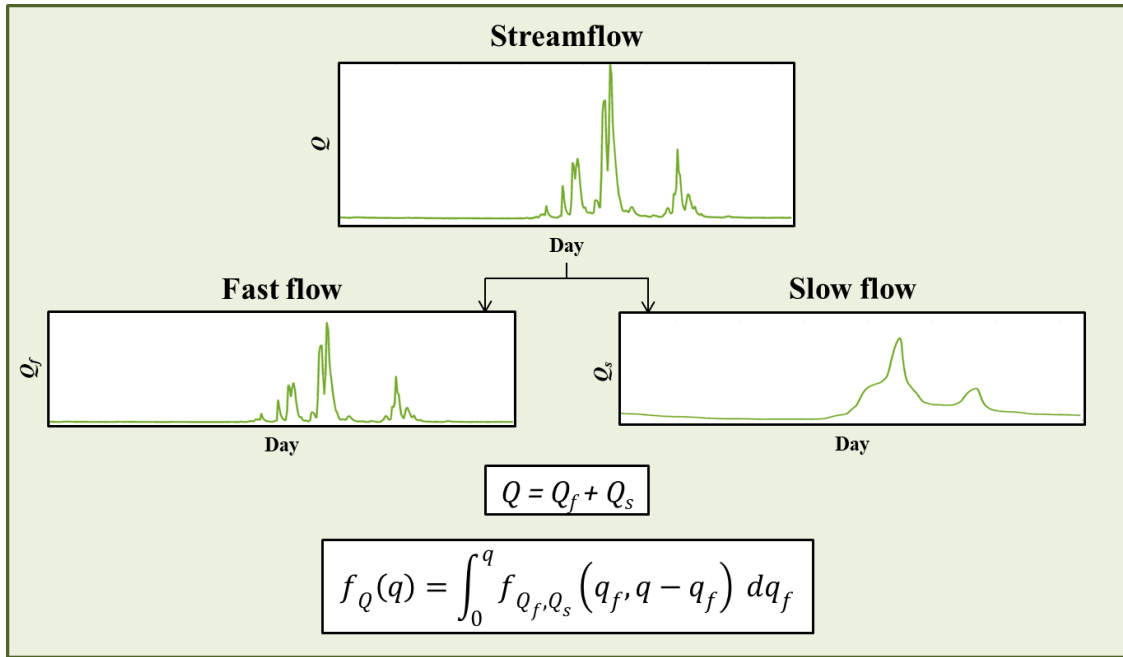
Figure S8. The schematic representation illustrates the process partitioning of streamflow time series into the fast flow and slow flow components (Ghotbi et al., 2020a).
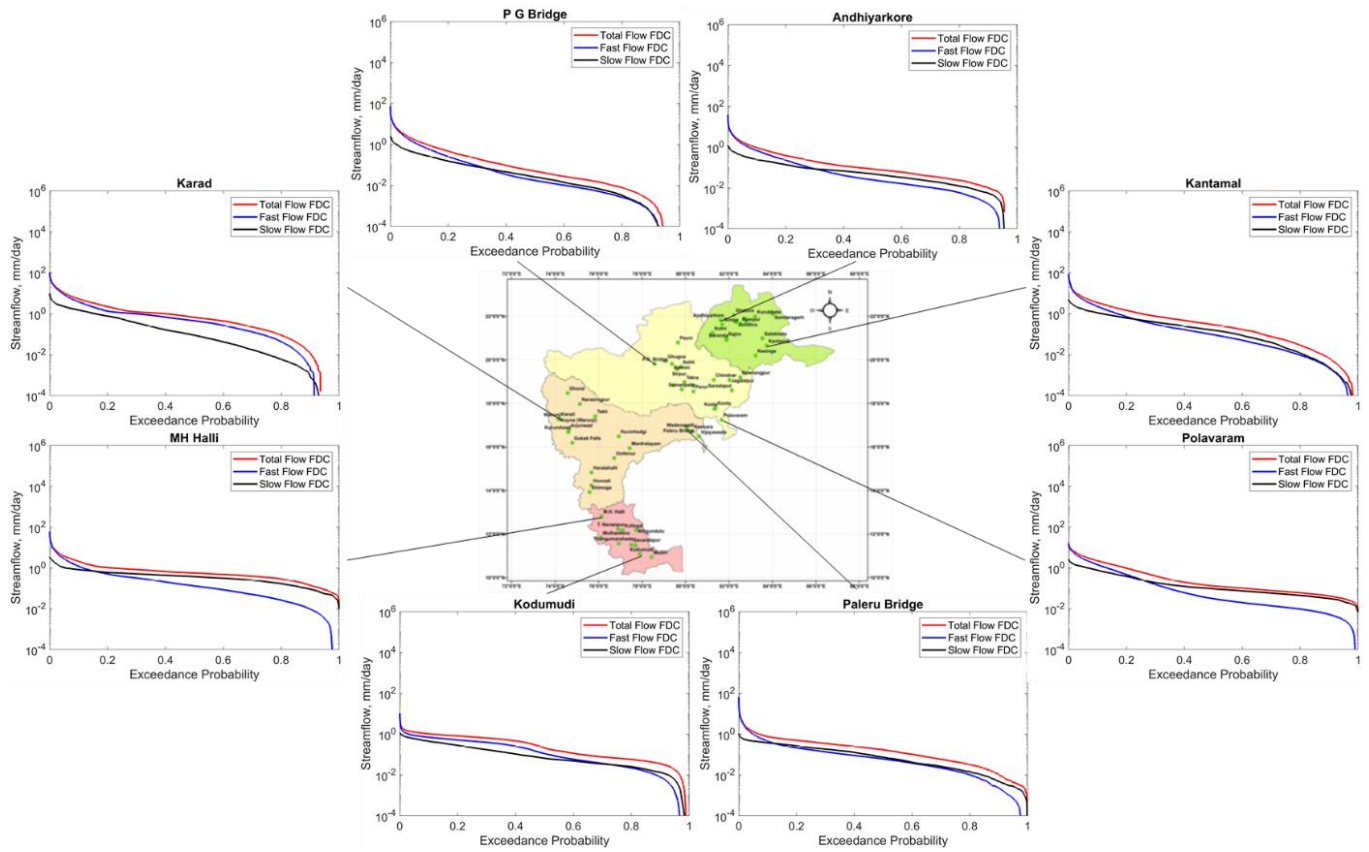
Figure S9: Spatial variation of slow, fast and total flow duration curves across Peninsular region. The fast and slow flow duration curves in the northern part of the region cut off after sustaining for 90% of the time. However, in the southern region, slow flow duration curves sustain throughout the entire duration, with magnitude higher than that of fast flow.
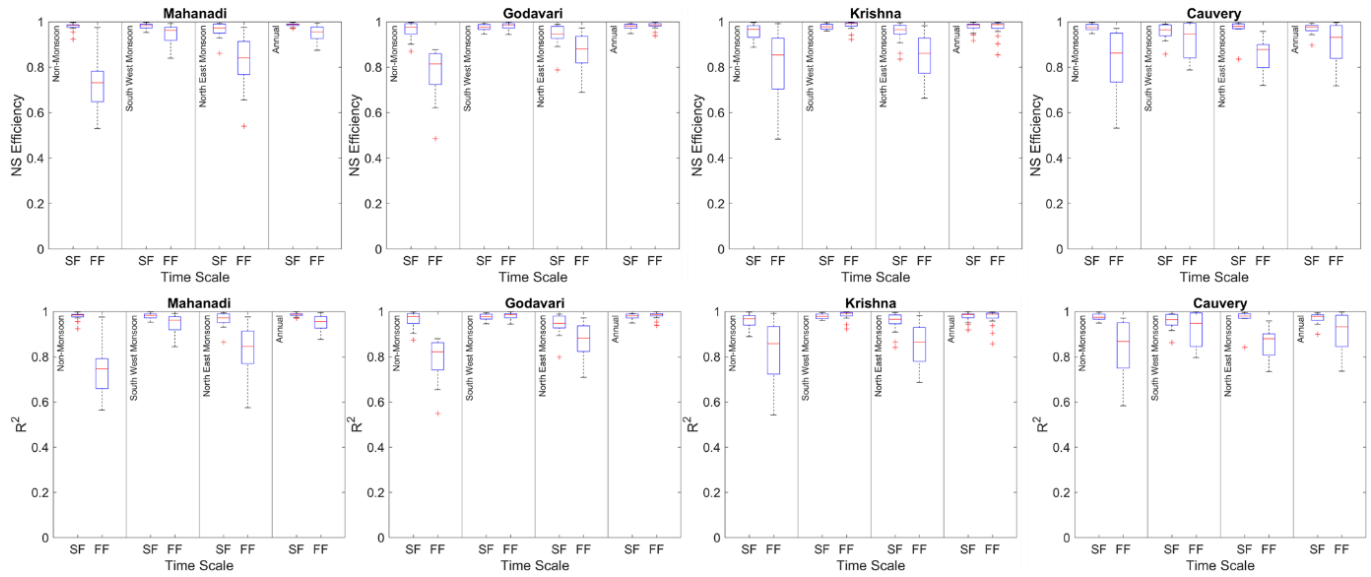
Figure S10: Goodness of fit of mixed gamma distribution for fast and slow flow components at seasonal scales. The values of coefficient of determination (R^2) and Nash-Sutcliffe efficiency (NSE) represent how well the observed flow duration curve is simulated using mixed gamma distribution model. It is observed that, the magnitude of R^2 of slow flow across all seasons is higher than that of fast flow. This is due to the fact that slow flow has higher residence time in the system which tend to reduce the variability in the flow dynamics. The nature of the geologic formations that supports the transmission of slow flow is one of the major factors controlling the slow flow variability. The performance of fast flow (R^2) is better during South-West monsoon season – the dominating season for streamflow generation.
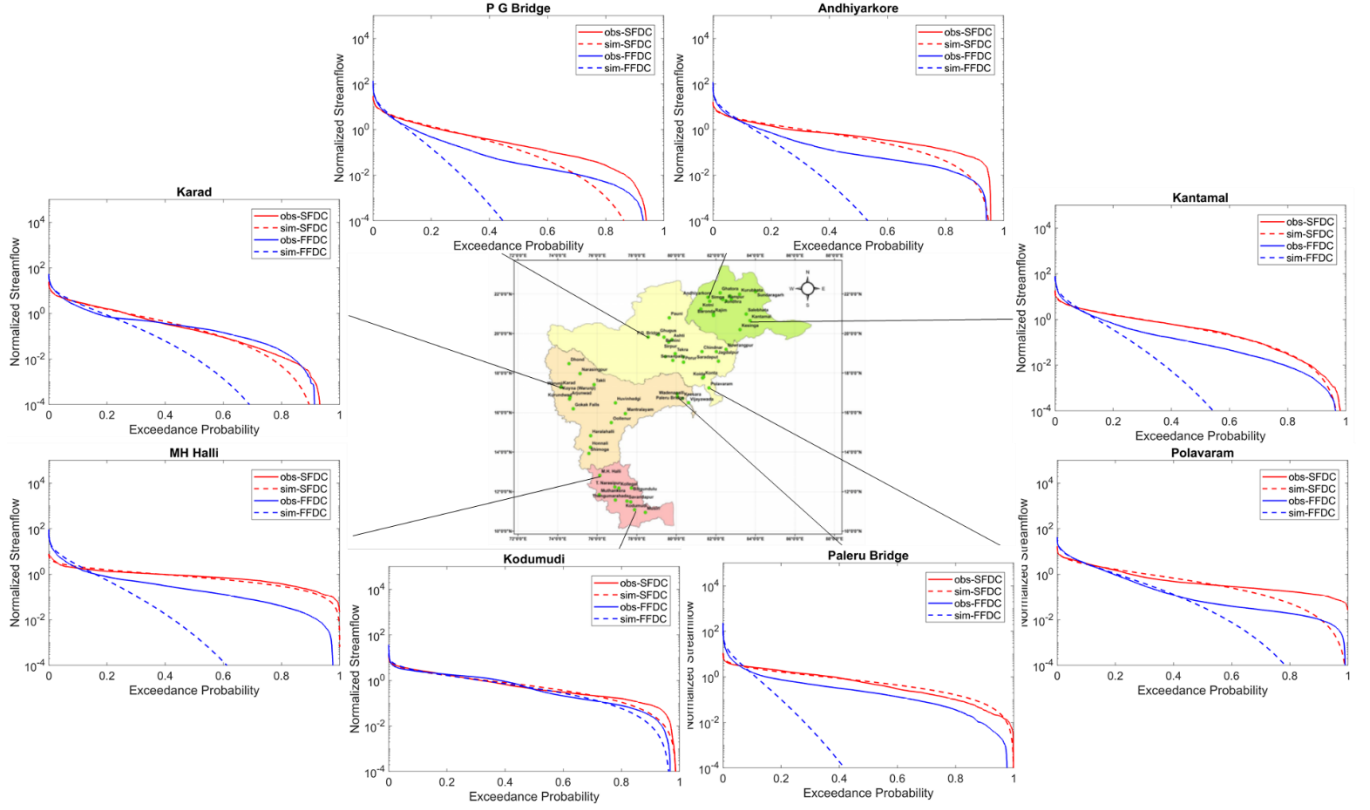
Figure S11: Normalized empirical FDCs and mixed gamma distribution fits for slow flow and fast flow. The logarithmic scale in y-axis tend to exaggerate the poor fits.

S2. Process partitioning

Daily streamflow is partitioned in such a way that it approximates the statistical summation of fast flow and slow flow at the daily scale:

$$Q = Q_f + Q_s \tag{S1}$$

where Q is the daily streamflow, Q_f is the daily fast flow, Q_s is the daily slow flow.

The relative contributions of fast flow ($C_{\rightarrow TF}$) and slow flow ($C_{SF \rightarrow TF}$) to total flow can be expressed as

$$C_{Q_f \rightarrow Q} = \frac{Total\ Fast\ Flow\ Volume}{Total\ Flow\ Volume} \tag{S2}$$

$$C_{Q_s \rightarrow Q} = \frac{Total\ Slow\ Flow\ Volume}{Total\ Flow\ Volume} \tag{S3}$$

Note that $C_{Q_f \rightarrow Q}$ and $C_{Q_s \rightarrow Q}$ effectively measure the relative contributions of fast and slow flows to the mean of the annual flow duration curve.

References

Jayaraman, A., Venkat Ratnam, M., Patra, A. K., Narayana Rao, T., Sridharan, S., Rajeevan, M., Gadhavi, H., Kesarkar, A. P., Srinivasulu, P. & Raghunath, K. (2010). Study of atmospheric forcing and responses (SAFAR) campaign : Overview. *Annales Geophysicae*. January 2010. https://doi.org/10.5194/angeo-28-89-2010.

Gaißer, S., Ruppert, M., & Schmid, F. (2010). A multivariate version of Hoeffding's Phi-Square. *Journal of Multivariate Analysis*, 101(10), 2571 2586.https://doi.org/10.1016/j.jmva.2010.07.006

Krishnamurthy, V., & Ajayamohan, R. S. (2010). Composite Structure of Monsoon Low Pressure Systems and Its Relation to Indian Rainfall. *Journal of Climate*, 23(16), 4285–4305. https://doi.org/10.1175/2010JCLI2953.1

Prakash, S., Mitra, A. K., & Pai, D. S. (2015). Comparing two high-resolution gauge-adjusted multisatellite rainfall products over India for the southwest monsoon period. *Meteorological Applications*, 22(3), 679–688. https://doi.org/10.1002/met.1502